A Probabilistic Approach to Power System Security Assessment under Uncertainty

D. D. Le, A. Berizzi, C. Bovo

Department of Energy,
Politecnico di Milano
Milan 20156, Italy

E. Ciapessoni, D. Cirio, A. Pitto

Ricerca sul Sistema Energetico - RSE
S.p.A.,
Milan, Italy

G. Gross

Department of Electrical and
Computer Engineering,
University of Illinois at Urbana-
Champaign
Urbana, IL 61801, USA

Abstract

The deepening penetration of renewable resources, such as wind and photovoltaic solar, has introduced additional uncertainty into power system operation and control. This added uncertainty, together with the conventional sources of uncertainty, the loads and the availability of resources and transmission assets, makes clear the limitations of the conventional deterministic power flow in power system analysis and security assessment applications. Therefore, the explicit consideration of uncertainty requires the deployment of probabilistic approaches so as to provide the ability to manage the wide spectrum of all possible values of the input and state variables. In this paper, we make use of cumulant-based probabilistic power flow methodology to account for correlations among the input random variables. Extensive testing indicates good performance of probabilistic power flow. We illustrate application of the probabilistic power flow on the 14-bus IEEE test system and present a comparison with the result obtained by the computationally more demanding Monte Carlo approach. The probabilistic power flow results provide valuable information for power system analysis and security assessment and, in particular, provide insights into issues associated with line overloading, over-/under-voltage, and the critical ramping requirements from conventional generators in system with deep penetration of highly variable resources, such as wind farms.

Introduction

The conventional deterministic power flow (DPF) is the most widely used tool in power system analysis, operations, planning and control. DPF uses the specified values of power generation and load, and the parameters of the network topology to compute system steady-state operating conditions without taking into account any sources of uncertainty affecting the power system. The deepening penetration of renewable energy sources (RES), such as wind and photovoltaic solar, has introduced additional uncertainty into power system operation and control. This added uncertainty along with the conventional sources of uncertainty, the loads and the availability of resources and transmission assets, makes clear the limitations of the conventional DPF in power system analysis and security assessment applications. In order to deal with the above

problems, a probabilistic approach needs to be used, where we explicitly represent the sources of uncertainty embedded by random variables ($r.v.$s). This approach is referred to as probabilistic power flow (PPF).

The early contribution in the PPF area was the scheme published in 1974 [1]. A general classification of PPF procedures is as follows: numerical methods and analytical methods. Monte Carlo Simulation (MCS) is a systematic methodology for the emulation of events under uncertainty [2]. The MCS for power flow studies under uncertainty uses multiple DPF solutions for the sampled values of the realizations of the $r.v.$s that are used to represent the various sources of uncertainty. The accuracy of the results is one of the advantages of this method and mostly depends on the number of samples [3], [4]. However, MCS is usually very computationally intensive. The basic idea of the analytical approach is to apply a defined algorithm, i.e., point estimate methods [5], [6], cumulant techniques [7], [8], or convolution techniques [9], [10] with probability density functions ($p.d.f.$s) and/or cumulative distribution functions ($c.d.f.$s) of $r.v.$s of inputs so that $p.d.f.$s and $c.d.f.$s of $r.v.$s of system states and line flows can be obtained. Point estimate methods are based on approximations: input variables are decomposed into a series of values and corresponding weights, and then the moments of the output variables of interest are computed as a function of the inputs. The cumulant methods adopt the properties of moments and cumulants, based on the probability distributions of input $r.v.$s and linearized power flow equations, while the convolution methods convolve all $r.v.$s. The conventional convolution technique or fast Fourier transform method requires more storage and computation time than cumulant methods.

In this paper, a cumulant-based PPF methodology is adopted. Correlation among nodal power injections from wind power generation and among loads is explicitly represented. In this way, the dependence of load/RES production forecast errors (e.g., due to weather forecast errors) over geographic areas can be taken into account. Also, the steady-state behaviour of the frequency regulation of conventional generation is included in the model. Hence, the control law of the generating units (e.g., secondary frequency regulation/AGC or tertiary frequency control, etc.) may be considered. In addition, PPF provides a complete spectrum of all possible values of generator power outputs, bus voltages, power flows, etc., in terms of $p.d.f.$s and

$c.d.f.$s so that they can be used for power system analysis and security assessment [11] and, in particular, issues associated with the critical ramping requirements from conventional generators, line overloading, and over-/under-voltage can be assessed with the eventual aim of planning control measures.

Probabilistic Power Flow with Distributed Slack Bus Model

Distributed Slack Bus Model

Traditionally, the slack bus is known in power flow computation as the bus which is responsible for balancing power mismatch in power system. However, in modern power system where the uncertainty of bus power injections is significant, for example, due to the stochastic nature of loads and wind power resources, the slack bus injection reflects the combination of uncertainty of all injections too. Nevertheless, in real power system operation, the actual power mismatch is usually shared by many generators, according to the frequency control. Consequently, the power output of all generators under frequency control will be affected by the uncertainty. Therefore, for such generators, it becomes difficult to assess both reserve margins and ramping constraint under uncertainty. The proposed approach can provide the useful information for dealing with this issue and for assessing power system security such as line overloading and over-/under-voltage as well.

The conventional DPF is based on the concept of a single slack bus due to the lack of prior knowledge of the losses in power system. In addition, this works well as far as the injections are known with good confidence. The slack bus is a mathematical model to take into account a priori uncertainty on losses; in the actual operation, however, the loading of generators is defined by the frequency control model. For example, in the very short-term, any imbalance is compensated by the droops of primary frequency regulators; in a longer term the same occurs for the participation factors of secondary frequency control (or AGC) and in an event longer term it can be done for tertiary control. In any case, any mismatch, or any uncertainty, can be allocated to some controlling generators, according to some participation factors α_i. The DPF model can be enhanced to take this into account, by the distributed slack model. With the distributed slack bus model (DSBM), any power mismatch (either due to uncertainty or to losses) can be assigned to a set of generating units participating in a real power allocation process, thus reflecting the actual operation in power system.

Let us assume that there are n buses in the power system; in the DSBM there is no more a 'slack bus', so 1 to m are the generator buses that take care of the overall real power imbalance in power system ΔP_{IB} while buses from $m+1$ to n (including load buses and remaining generator buses) are not involved in the imbalance sharing. In DSBM, modification in the formulation is only relevant to the real power part of the Jacobian matrix as follows [12], [13]

$$
\begin{bmatrix} \Delta P_1 \\ \Delta P_2 \\ \vdots \\ \Delta P_m \\ \Delta P_{m+1} \\ \vdots \\ \Delta P_n \end{bmatrix} = \begin{bmatrix} \frac{\partial P_1}{\partial P_{IB}} & \frac{\partial P_1}{\partial \theta_2} & \cdots & \frac{\partial P_1}{\partial \theta_m} & \frac{\partial P_1}{\partial \theta_{m+1}} & \cdots & \frac{\partial P_1}{\partial \theta_n} \\ \frac{\partial P_2}{\partial P_{IB}} & \frac{\partial P_2}{\partial \theta_2} & \cdots & \frac{\partial P_2}{\partial \theta_m} & \frac{\partial P_2}{\partial \theta_{m+1}} & \cdots & \frac{\partial P_2}{\partial \theta_n} \\ \vdots & \vdots & & \vdots & \vdots & & \vdots \\ \frac{\partial P_m}{\partial P_{IB}} & \frac{\partial P_m}{\partial \theta_2} & \cdots & \frac{\partial P_m}{\partial \theta_m} & \frac{\partial P_m}{\partial \theta_{m+1}} & \cdots & \frac{\partial P_m}{\partial \theta_n} \\ 0 & \frac{\partial P_{m+1}}{\partial \theta_2} & \cdots & \frac{\partial P_{m+1}}{\partial \theta_m} & \frac{\partial P_{m+1}}{\partial \theta_{m+1}} & \cdots & \frac{\partial P_{m+1}}{\partial \theta_n} \\ \vdots & \vdots & & \vdots & \vdots & & \vdots \\ 0 & \frac{\partial P_n}{\partial \theta_2} & \cdots & \frac{\partial P_n}{\partial \theta_m} & \frac{\partial P_n}{\partial \theta_{m+1}} & \cdots & \frac{\partial P_n}{\partial \theta_n} \end{bmatrix} \begin{bmatrix} \Delta P_{IB} \\ \Delta \theta_2 \\ \vdots \\ \Delta \theta_m \\ \Delta \theta_{m+1} \\ \vdots \\ \Delta \theta_n \end{bmatrix} \quad (1)
$$

Each element of the first column of the modified Jacobian matrix is the participation factor of each generator in the real power allocation process and zero otherwise [12]:

$$
\frac{\partial P_i}{\partial P_{IB}} = \alpha_i \quad (2)
$$

$$
\sum_i^m \alpha_i = 1 \quad (3)
$$

An iterative process is then adopted to solve the real power flow equations (1) and after each iteration, the voltage magnitudes, voltage angles and also the imbalance are updated (by solving the reactive subproblem according to the conventional model).

For a convergent power flow, the amount of real power imbalance in power system is distributed among generators based on participation factors α_i so that their real power outputs can be represented as

$$
P_{Gi} = P_{Gi0} + \alpha_i\,\Delta IB \quad (4)
$$

$$
P_{Gi}^{\,low} \leq P_{Gi} \leq P_{Gi}^{\,up} \quad (5)
$$

where
  P_{Gi} is the real power output of generators connected to bus i,
  P_{Gi0} is the scheduled real power output of generating units connected to bus i,
  ΔIB is the total real power imbalance at solution point (the difference between the schedules of generators and their outputs computed by a DPF with DSBM),
  $P_{Gi}^{\,up}$ and $P_{Gi}^{\,low}$ are the upper and lower limits of the ith real power generation, respectively.

The participation factors in the general model above can be defined depending on the considered time frame. In particular, taking the secondary frequency regulation time frame as an example, the participation factors can be calculated as

$$\alpha_i = \frac{agc_i}{agc_\Sigma} \tag{6}$$

$$agc_\Sigma = \sum_i^m agc_i \tag{7}$$

$$P_{Gi} + agc_i^{max} \leq P_{Gi}^{max} \tag{8}$$

$$P_{Gi} - agc_i^{min} \geq P_{Gi}^{min} \tag{9}$$

where

agc_Σ is total system AGC requirement according to secondary frequency regulation (MW),

agc_i is the accepted AGC quantity by generating units at bus i,

$agc_i^{max} \geq 0$ and $agc_i^{min} \geq 0$ are the regulation limits (the capacity limits due to unit characteristics),

P_{Gi}^{max} is the maximum real power generation (physical limit),

P_{Gi}^{min} is the minimum real power generation.

Distributed Slack Probabilistic Power Flow

The basic power flow equations can be expressed in general in a matrix form as [14], [15]:

$$\boldsymbol{w} = g(\boldsymbol{x}) \tag{10}$$

$$\boldsymbol{z} = h(\boldsymbol{x}) \tag{11}$$

where

$\boldsymbol{w}$ is the vector of nodal injected powers,
$\boldsymbol{x}$ is the vector of state variables,
$\boldsymbol{z}$ is the vector of line power flows,
and
$g(\boldsymbol{x})$ are the power flow equations,
$h(\boldsymbol{x})$ are the functions to compute line power flows.

With DSBM [12], equation (10) can be rewritten as:

$$\boldsymbol{w} = g(\begin{bmatrix} P_{IB} \\ \boldsymbol{x} \end{bmatrix}) \tag{12}$$

It should be noted that vector $\boldsymbol{w}$ in (12) includes the power injections of all buses in the power system while in (10), power injections at the slack bus is not included.

The solution is obtained by solving a DPF for DSBM. Using Taylor series expansion to linearize the above equations around the solution point gives [14]

$$\Delta w = \begin{bmatrix} \boldsymbol{J_0} \end{bmatrix} \begin{bmatrix} \Delta IB \\ \Delta \boldsymbol{x} \end{bmatrix} \tag{13}$$

so

$$\begin{bmatrix} \Delta IB \\ \Delta \boldsymbol{x} \end{bmatrix} = \begin{bmatrix} \boldsymbol{S_0} \end{bmatrix} \Delta w \tag{14}$$

$$\Delta z = \begin{bmatrix} \boldsymbol{T_0} \end{bmatrix} \Delta w \tag{15}$$

where $[\boldsymbol{S_0}]$ is the inverse of modified Jacobian matrix $[\boldsymbol{J_0}]$ and $[\boldsymbol{T_0}]$ is the sensitivity matrix of power flows with respect to nodal power injections at the solution point.

To solve the PPF, $\boldsymbol{w}$, $\boldsymbol{x}$, $\boldsymbol{z}$ elements and IB are assumed as $r.v.$s. From relationships in (14) and (15), a cumulant-based PPF [8], [14], [15] can be adopted. Moreover, for taking into account the correlation among input $r.v.$s, the joint cumulant described in [15] is used.

If $r.v.$ y is a linear combination of r $r.v.$s $u_i, i = 1, \ldots, r$:

$$y = a_1 u_1 + a_2 u_2 + \cdots + a_r u_r \tag{16}$$

the cumulants of y can be calculated from the cumulants of u_i as follows [15]

$$
\begin{aligned}
y^{(1)} &= E(\sum_{i=1}^r a_i u_i) = \sum_{i=1}^r a_i u_i^{(1)} \\
y^{(2)} &= E[(\sum_{i=1}^r a_i u_i)^2] - [E(\sum_{i=1}^r a_i u_i)]^2 \\
&= \sum_{i=1}^r a_i^2 u_i^{(2)} + 2 \sum_{i=1, i<j}^r a_i a_j u_{(i^{(1)}, j^{(1)})} \\
y^{(3)} &= E[(\sum_{i=1}^r a_i u_i)^3] - 3E(\sum_{i=1}^r a_i u_i) E[(\sum_{i=1}^r a_i u_i)^2] \\
&\quad + 2[E(\sum_{i=1}^r a_i u_i)]^3 \\
&= \sum_{i=1}^r a_i^3 u_i^{(3)} + 3 \sum_{i=1, i \neq j}^r a_i^2 a_j u_{(i^{(2)}, j^{(1)})} \\
&\quad + 6 \sum_{i=1, i<j<l}^r a_i a_j a_l u_{(i^{(1)}, j^{(1)}, l^{(1)})} \cdots \\
&\vdots
\end{aligned} \tag{17}
$$

where

$E(\cdot)$ is the mathematical expectation operator,

$y^{(k)}$ and $u_i^{(k)}$ are the kth order cumulant of y and u_i, respectively,

$u_{(i^{(k_i)},j^{(k_j)},l^{(k_l)},\dots)}$ is the kth order joint cumulant with $k = k_i + k_j + k_l + \cdots$ of $r.v.$s u_i, u_j, u_l, ...

If $r.v.$s u_1, u_2, ..., u_r are independent, the kth order cumulant of y can simply be obtained as:

$$y^{(k)} = a_1^k\, u_1^{(k)} + a_2^k\, u_2^{(k)} + \cdots + a_r^k\, u_r^{(k)} \qquad (18)$$

In particular, in case of two $r.v.$s u_i and u_j, the second order joint cumulants are calculated as:

$$
\begin{aligned}
u_{(i^{(2)},j^{(0)})} &= \sigma_{u_i}^2 \\
u_{(i^{(0)},j^{(2)})} &= \sigma_{u_j}^2 \\
u_{(i^{(1)},j^{(1)})} &= \rho_{u_i,u_j}\, \sigma_{u_i}\, \sigma_{u_j}
\end{aligned}
\qquad (19)
$$

where

σ is the standard deviation,

ρ_{u_i,u_j} is correlation coefficient between u_i and u_j, calculated as

$$\rho_{u_i,u_j} = \frac{cov(u_i,\,u_j)}{\sigma_{u_i}\,\sigma_{u_j}} = \frac{E[(u_i - \mu_{u_i})(u_j - \mu_{u_j})]}{\sigma_{u_i}\,\sigma_{u_j}} \qquad (20)$$

where

$cov(u_i,\,u_j)$ is the covariance between u_i and u_j,

μ_{u_i} and μ_{u_j} are the means (expected values) of u_i and u_j, respectively,

$|\rho_{u_i,u_j}| \le 1$; if $\rho_{u_i,u_j} = 0$, u_i and u_j are independent; if $\rho_{u_i,u_j} = 1$, u_i and u_j are perfectly positively dependent; if $\rho_{u_i,u_j} = -1$, u_i and u_j are perfectly negatively dependent.

The procedure for the cumulant-based Distributed Slack PPF (DSPPF) is as follows

- Run DPF with DSBM to obtain the expected values x_0, z_0, and IB_0 and the sensitivity matrices $[S_0]$ and $[T_0]$.
- Calculate the self and joint cumulants [8], [14], [15] of nodal power injections.
- Compute cumulants of state variables, line power flows, and total imbalance using (14), (15), and (17).
- Calculate cumulants of power outputs of generators based on (4).
- From cumulants, $p.d.f.$s and/or $c.d.f.$s of the output of interest can be obtained by using, for example, Gram-Charlier series expansion [8], or Edgeworth expansion, Cornish-Fisher expansion [15], Von Mises function [7] and so on, depending on the type of distributions considered.
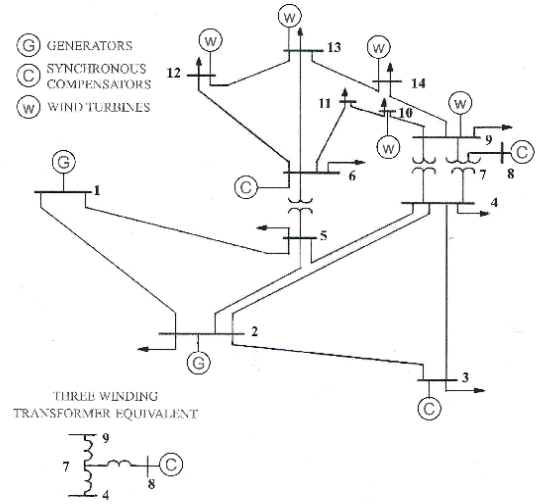

Fig. 1: Modified IEEE 14-bus Test System

From $p.d.f.$s and $c.d.f.$s obtained by DSPPF, the probability of line overloading, over-/under-voltage, and the risk of critical ramping and overloading of generators can be calculated and assessed, e.g., for the next hour, based on the forecast, the electricity market output, etc.

Numerical Results

We illustrate the application of the proposed approach to a case study on the modified IEEE 14-bus test system. The single line diagram, branch, bus, and generator data of the IEEE 14-bus test system are presented in [10], [16]. However, in the present research, five wind farms were added to the system at buses 9, 10, 12, 13, and 14 with the nominal power of 27, 15, 12, 15, and 21 MW, respectively, as depicted in Fig. 1. The information of wind power production, load, and their uncertainties for a considered look-ahead horizon are assumed to be known by forecast techniques. The information about correlation among load/wind production are assumed as well and could also be obtained by time-series techniques. Nevertheless, they are beyond the scope of this paper. Here, we assume that a forecast technique is available and provides a 15-minute (or other time steps) sequence of load and wind production forecasts, their expected forecast errors and correlations during the considered scheduling horizon. For the sake of simplicity, the forecast errors are assumed normally distributed but it is possible to adopt other distributions. In addition, the scheduled power output of generators are assumed to be known. In the system, generators at bus 1 (G1) and 2 (G2) are slack distributed so that, in any case, the power imbalance is shared among them with corresponding participation factors and according to the frequency control.

Let us assume that at time t_0 a forecast for both wind and loads is available for time t_k and $t_{k+1} = t_k + \Delta t$. Depending on the time frame considered, the value for t_k can range from one hour to a dozen of hours, as well as the Δt values can range from 5 minutes to an hour. Of course, according to the

TABLE I: Wind power forecasts at time step t_k

bus	9	10	12	13	14
wind power (MW)	24	12	9	12	18
error (%)	12	12	12	12	12

TABLE II: Correlation coefficients among loads

bus	2	3	4	5	6	9	10	11	12	13	14
2	1.00	0.15	0.15	0.15	0.05	0.05	0.05	0.05	0.05	0.05	0.05
3	-	1.00	0.15	0.15	0.05	0.05	0.05	0.05	0.05	0.05	0.05
4	-	-	1.00	0.15	0.05	0.05	0.05	0.05	0.05	0.05	0.05
5	-	-	-	1.00	0.05	0.05	0.05	0.05	0.05	0.05	0.05
6	-	-	-	-	1.00	0.20	0.20	0.20	0.05	0.05	0.05
9	-	-	-	-	-	1.00	0.20	0.20	0.05	0.05	0.05
10	-	-	-	-	-	-	1.00	0.20	0.05	0.05	0.05
11	-	-	-	-	-	-	-	1.00	0.05	0.05	0.05
12	-	-	-	-	-	-	-	-	1.00	0.20	0.20
13	-	-	-	-	-	-	-	-	-	1.00	0.20
14	-	-	-	-	-	-	-	-	-	-	1.00

TABLE III: Wind power forecasts at time step t_{k+1}

bus	9	10	12	13	14
wind power (MW)	25	14	10	14	20
error (%)	15	15	15	15	15

TABLE IV: Real power schedules (MW) at the considered time steps

bus	1	2
t_k	235	30
t_{k+1}	253	46

time frame considered, the values of uncertainty are likely to be very different; however, the model can take into account all these cases; in the present paper, just an application is shown. Assume that for time t_k the information about wind power forecast is provided as in Table I. The forecast errors are assumed normally distributed represented in terms of standard deviation (in %) from the mean. In this test, the correlation coefficients among wind resources are assumed to be 0.5 and those among loads are shown in Table II.

For the next time step t_{k+1}, load of power system is assumed to be increased 10 % and the forecasting error is kept equal while wind power forecasts are provided as in Table III. The power outputs of dispatchable generators at bus 1 and 2 are assumed as in Table IV.

The proposed method is presented here with reference to the evaluation of security at times t_k and t_{k+1}, as well as for ramping constraint evaluation between times t_k and t_{k+1}. At the same time, in order to assess the accuracy of the proposed method, a MCS with 30,000 samples has been carried out and taken as reference. The Average Root Mean Square ($ARMS$) error is computed to compare the DSPPF and the MCS results. $ARMS$ is defined as:
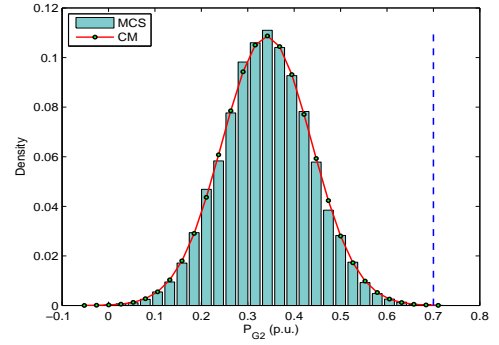
Fig. 2: $p.d.f.$ curves of P_{G2} at time step t_k

$$ARMS = \frac{\sqrt{\sum\limits_{i=1}^{N}(MCS_i - DSPPF_i)^2}}{N} \qquad (21)$$

where MCS_i and $DSPPF_i$ are the ith value on $c.d.f.$ curves obtained by MCS and DSPPF, respectively. N is the number of samples considered in the range of the $c.d.f.$s.

The $c.d.f.$s and/or $p.d.f.$s of generator power outputs, power flows, and voltages can be obtained by the proposed DSPPF. The power imbalance in the system is shared by G1 and G2 according to their participation factors. For instance, at time step t_{k+1}, the imbalance between schedules of generators (Table IV) and their outputs computed according to a DPF with DSBM is 1.55 MW. This imbalance depending on losses, is shared among G1 and G2 with $\alpha_1 = 0.42$ and $\alpha_2 = 0.58$, resulting in the following expected values: $P_{G1} = 253.65$ MW and $P_{G2} = 46.90$ MW. At this point, the probabilistic part of the DSPPF is carried out, resulting in $p.d.f.$s shown in Fig. 2 and 3 for P_{G2} at time steps t_k and t_{k+1}, respectively. It is interesting that the curves obtained by the proposed method are very close to the results obtained by MCS: the $ARMS$ values are 2.62×10^{-2} % and 1.57×10^{-2} %, respectively. The expected values of P_{G2} at t_k and t_{k+1} are 0.341 and 0.469 p.u. (in this test, the base power of 100 MVA is used), respectively; they take into account both the share of the losses (deterministic amount) and the uncertainties on both wind generation and loads (with correlation), that provide the shape of the $p.d.f.$s.

Based on the output of the PPFs, we can first assess the risk of over-/under-regulation limits. Assume that the upper regulation limit of generator G2 is 0.7 p.u. (the vertical line in Fig. 2 and 3): we can calculate the probability that P_{G2} is higher than its upper limit as

$$
\begin{aligned}
t_k &: P(P_{G2} > 0.7) = 0 \\
t_{k+1} &: P(P_{G2} > 0.7) = 0.031
\end{aligned}
\qquad (22)
$$

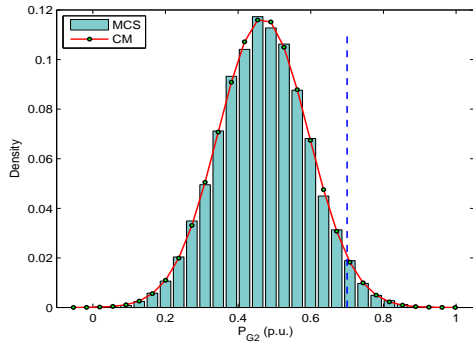Moreover, output of DSPPF allows us to evaluate the risk of

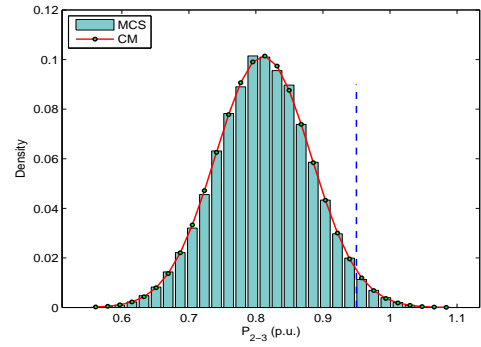Fig. 3: $p.d.f.$ curves of P_{G2} at time step t_{k+1}

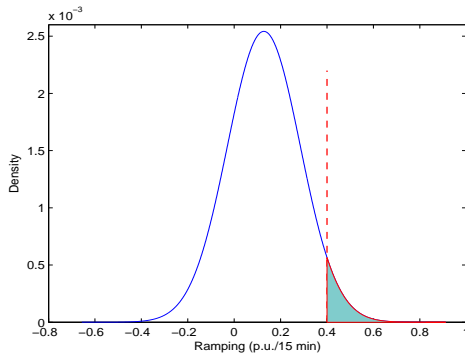

Fig. 6: $p.d.f.$ curves of P_{2-3} at time step t_{k+1}

Fig. 4: Ramping of P_{G2}
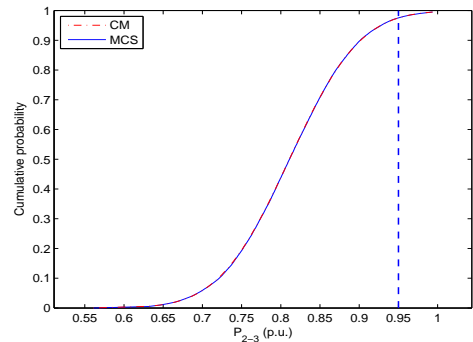

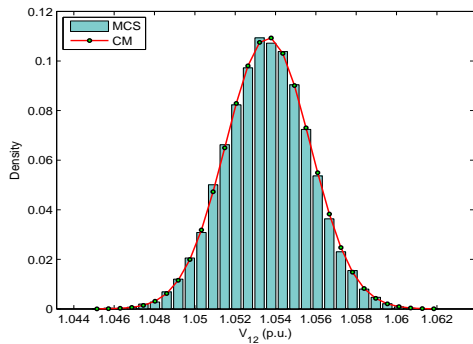
Fig. 7: $c.d.f.$ curves of P_{2-3} at time step t_{k+1}

Fig. 5: $p.d.f.$ curves of V_{12} at time step t_{k+1}

thermal rating) of line 2-3, for instance, is 0.95 p.u. (the vertical line in Fig. 6 and 7), then the probability being greater than its upper bound is zero at t_k, but at t_{k+1} is 0.025, mainly due to the increase of load. In this test, as the operating range of voltage at bus 12 is [0.94, 1.06] p.u., voltage at bus 12 is within the range. The $ARMS$ calculated for V_{12} and P_{2-3} above are 2.86×10^{-2} % and 9.83×10^{-3} %, respectively, showing the very good accuracy of the proposed method.

Conclusions

In this paper, a cumulant-based probabilistic power flow methodology accounting for correlations among input random variables is adopted to provide full spectrum of all possible values of the desired variables for power system security assessment under uncertainty. A probabilistic power flow with distributed slack bus model is developed so that any power imbalance in power system can be charged to a set of dispatchable generators, for example, as a response to a signal from the secondary frequency regulation, so reflecting the actual power system operation.

The proposed approach is able to assess power system security in terms of such as line overloading, over-/under-voltage and, in particular, to evaluate the risk of critical ramping and over-/under-regulation limits of generators in systems with deep penetration of highly variable resources, such as wind farms.

critical ramping for generator G2 from time step t_k to time step t_{k+1}, of course, depending on $\Delta t = t_{k+1} - t_k$. For example, if $\Delta t = 15$ minutes, from the distributions of power output at the two time steps, the $p.d.f.$ of ramping can be obtained as in Fig. 4. Analogously, assume that the maximum ramp rate for increasing the output of G2 is 0.4 p.u./15 min (the vertical line in Fig. 4): the probability that the ramp is higher than its upper bound is 0.02 (the filled area in Fig. 4).

For illustration of power flow and voltage assessments, the $p.d.f.$s and/or $c.d.f.$s of a selected voltage at bus 12 (V_{12}) and real power flow through line 2-3 (P_{2-3}) at t_{k+1} are presented in Fig. 5 to 7, respectively.

If the upper bound of the real power flow (e.g., owing to

Acknowledgment

References

[1] B. Borkowska, "Probabilistic load flow," *IEEE Trans. Power App. Syst.*, vol. PAS-93, no. 4, pp. 752-759, Apr. 1974.

[2] J. M. Hammenley and D. C. Handscomb, *Monte Carlo Methods*. Norwich: Fletcher and Son Ltd, 1964.

[3] M. Delfanti, C. Bovo, M. S. Pasquadibisceglie, M. Pozzi, E. Zio, "Indirect Monte Carlo Approach to Evaluate Reliability and Availability Indices of Distribution Networks", *18th International Conference and Exhibition on Electricity Distribution, CIRED 2005*, pp. 1-5, 2005.

[4] A. Berizzi, C. Bovo, M. Delfanti, M. Merlo, and M. S. Pasquadibisceglie, "A Monte Carlo Approach for TTC Evaluation," *IEEE Trans. Power Syst.*, vol. 22, no. 2, pp. 735-743, 2003.

[5] C. L. Su, "Probabilistic load-flow computation using point estimate method," *IEEE Trans. Power Syst.*, vol. 20, no. 4, pp. 1843-1851, Nov. 2005.

[6] J. M. Morales and J. Perez-Ruiz, "Point Estimate Schemes to Solve the Probabilistic Power Flow," *IEEE Trans. Power Syst.*, vol. 22, no. 4, pp. 1594-1601, 2007.

[7] L. A. Sanabria and T. S. Dillon, "Stochastic power flow using cumulants and Von Mises functions," *Elect. Power Energy Syst.*, vol. 8, no. 1, pp. 47-60, Jan. 1986.

[8] P. Zhang and S. T. Lee, "Probabilistic load flow computation using the method of combined cumulants and Gram-Charlier expansion," *IEEE Trans. Power Syst.*, vol. 19, no. 1, pp. 676-682, Feb. 2004.

[9] R. N. Allan and M. R. G. Al-Shakarchi, "Probabilistic a.c. load flow", *Proceedings of the Institution of Electrical Engineers*, vol. 123, no. 6, pp. 531-536, Jun. 1976.

[10] R. N. Allan and M. R. G. Al-Shakarchi, "Probabilistic techniques in a.c. load-flow analysis", *Proceedings of the Institution of Electrical Engineers*, vol. 124, no. 2, pp. 154-160, Feb. 1977.

[11] A. Berizzi, C. Bovo, E. Fumagalli, and E. A. Grimaldi, "Security Assessment in Operation: A Comparative Study of Probabilistic Approach", *Power Tech Conference Proceedings, IEEE*, vol. 1, Bologna, Jun. 2003.

[12] A. Zobian and M. D. Ilic, "Unbundling of Transmission and Ancillary Services. I. Technical Issues," *IEEE Trans. Power Syst.*, vol. 12, no. 2, pp. 539-548, May. 1997.

[13] A. Berizzi, C. Bovo, M. Delfanti, M. Merlo, and F. Tortello, "Singular Value Decomposition for an ORPF Formulation in Presence of SVR," *Electrotecnical Conference MELECON IEEE*, pp. 968-972, Mediterranean, 2006.

[14] D. D. Le, C. Bovo, A. Berizzi, E. Ciapessoni, D. Cirio, and A. Pitto, "A Detailed Comparison of Cumulant-based Probabilistic Power Flow Methods," *International Review of Electrical Engineering*, vol. 7, no. 1, pp. 3562-3573, Feb. 2012.

[15] M. Fan, V. Vittal, G. T. Heydt, and R. Ayyanar, "Probabilistic Power Flow Studies for Transmission Systems With Photovoltaic Generation Using Cumulants," *IEEE Trans. Power Syst.*, vol. 27, no. 4, pp. 2251-2261, Nov. 2012.

[16] R. Christie, Power system test case archive, Aug. 1993, *[Online]* http://www.ee.washington.edu/research/pstca.